JOURNAL OF THE AMERICAN COLLEGE OF CARDIOLOGY VOL. 77, NO. 13, 2021

ORIGINAL INVESTIGATIONS

Eruptive Calcified Nodules as a Potential Mechanism of Acute Coronary Thrombosis and Sudden Death

Sho Torii, MD, PhD,[a,*] Yu Sato, MD,[a,*] Fumiyuki Otsuka, MD,[a,b] Frank D. Kolodgie, PhD,[a] Hiroyuki Jinnouchi, MD,[a] Atsushi Sakamoto, MD, PhD,[a] Joohyung Park, MD,[a] Kazuyuki Yahagi, MD,[a] Kenichi Sakakura, MD,[a] Anne Cornelissen, MD,[a] Rika Kawakami, MD,[a] Masayuki Mori, MD,[a] Kenji Kawai, MD,[a] Falone Amoa, MD,[a] Liang Guo, PhD,[a] Matthew Kutyna, MS,[a] Raquel Fernandez, BS,[a] Maria E. Romero, MD,[a] David Fowler, MD,[c] Aloke V. Finn, MD,[a,d] Renu Virmani, MD[a]

ABSTRACT

BACKGROUND Calcified nodule (CN) has a unique plaque morphology, in which an area of nodular calcification causes disruption of the fibrous cap with overlying luminal thrombus. CN is reported to be the least frequent cause of acute coronary thrombosis, and the pathogenesis of CN has not been well studied.

OBJECTIVES The purpose of this study is to provide a comprehensive morphologic assessment of the CN in addition to providing an evolutionary perspective as to how CN causes acute coronary thrombosis in patients with acute coronary syndromes.

METHODS A total of 26 consecutive CN lesions from 25 subjects from our autopsy registry were evaluated. Detailed morphometric analysis was performed to understand the plaque characteristics of CN and nodular calcification.

RESULTS The mean age was 70 years, with a high prevalence of diabetes and chronic kidney disease. CNs were equally distributed between men and women, with 61.5% of CNs found in the right coronary artery (n = 16), mainly within its mid-portion (56%). All CNs demonstrated surface nonocclusive luminal thrombus, consisting of multiple nodular fragments of calcification, protruding and disrupting the overlying fibrous cap, with evidence of endothelial cell loss. The degree of circumferential sheet calcification was significantly less in the culprit section (89° [interquartile range: 54° to 177°]) than in the adjacent proximal (206° [interquartile range: 157° to 269°], p = 0.0034) and distal (240° [interquartile range: 178° to 333°], p = 0.0004) sections. Polarized picrosirius red staining showed the presence of necrotic core calcium at culprit sites of CNs, whereas collagen calcium was more prevalent at the proximal and distal regions of CNs.

CONCLUSIONS Our study suggests that fibrous cap disruption in CN with overlying thrombosis is initiated through the fragmentation of necrotic core calcifications, which is flanked—proximally and distally—by hard, collagen-rich calcification in coronary arteries, which are susceptible to mechanical stress. (J Am Coll Cardiol 2021;77:1599-611)

Listen to this manuscript's audio summary by Editor-in-Chief Dr. Valentin Fuster on JACC.org.

From the [a]CVPath Institute, Gaithersburg, Maryland, USA; [b]National Cerebral and Cardiovascular Center, Department of Cardiovascular Medicine, Osaka, Japan; [c]Office of the Chief Medical Examiner, Baltimore, Maryland, USA; and the [d]University of Maryland, School of Medicine, Baltimore, Maryland, USA. *Drs. Torii and Sato contributed equally to this work.
The authors attest they are in compliance with human studies committees and animal welfare regulations of the authors' institutions and Food and Drug Administration guidelines, including patient consent where appropriate. For more information, visit the Author Center.

Manuscript received October 23, 2020; revised manuscript received January 21, 2021, accepted February 1, 2021.

ISSN 0735-1097/$36.00 https://doi.org/10.1016/j.jacc.2021.02.016

ABBREVIATIONS AND ACRONYMS

ACS = acute coronary syndromes

CKD = chronic kidney disease

CN = calcified nodule

DM = diabetes mellitus

IVUS = intravascular ultrasound

NC = necrotic core

OCME = Office of the Chief Medical Examiner

OCT = optical coherence tomography

SCD = sudden cardiac death

SCoD = sudden coronary death

Coronary heart disease is the leading cause of mortality in the United States, accounting for one-third of all deaths in subjects above 35 years of age. Acute luminal thrombosis in the coronary artery is one of the main causes of sudden cardiac death (SCD) (1). We have reported in 2000 and 2015, that individuals presenting with sudden coronary death without previous histories of coronary heart disease had acute thrombosis in more than 50% of cases (2,3). The most common causes of acute coronary thrombosis are plaque rupture (65%), which is most commonly found in men <50 years of age, followed by plaque erosion (30%), which most frequently occurs in young women (<50 years); the least frequent cause is calcified nodule (CN) (5%) (3). We defined CN as "a lesion with fibrous cap disruption and luminal thrombus associated with eruptive, dense, calcific nodules" (2). Since our first publication in 2000, we have a more thorough understanding because of new methods used to better elucidate the underlying mechanisms that contribute to its occurrence.

SEE PAGE 1612

Unlike CN, lesion morphology of plaque ruptures and plaque erosions have been well described in several pathologic and clinical studies (4–14). For plaque rupture, a disruption of the thin fibrous cap overlying a necrotic core (NC) is considered the trigger for thrombus formation (4–9), whereas in plaque erosion, there is an acute luminal thrombus in direct contact with the intima, which exhibits an absence of endothelial cells (7–14). However, for CNs, it is clear that these lesions are more frequently seen in older persons; both the mechanisms by which these lesions develop and the type of underlying plaques leading to the formation of a CN remain unclear. Moreover, despite recent advances in intravascular imaging modalities, such as intravascular ultrasound (IVUS) and optical coherence tomography (OCT), that enable us to diagnose plaque characteristics in living patients with acute coronary syndromes (ACS) (15–21), such techniques have limited resolution for a detailed characterization of CN. The purpose of this study is to provide a comprehensive morphologic assessment of the CN in addition to providing an evolutionary perspective as to how this least frequent—yet still lethal—condition causes acute coronary thrombosis in patients with ACS.

TABLE 1 Clinical Characteristics and Risk Factors of Cases With Calcified Nodule

Patient characteristics	(n = 25)
Age, yrs	70.0 ± 12.6
Female	12 (48)
Race	
White	20 (80)
Black	4 (16)
others	1 (4)
Body height, cm	169.2 ± 14.1
Body weight, kg	75.6 ± 21.7
Body mass index, kg/m^2	26.1 ± 5.5
Patient risk factors*	
Hypertension	17/19 (89)
Diabetes	11/19 (58)
Smoking	8/19 (42)
Hyperlipidemia	7/19 (37)
Chronic kidney disease	10/19 (53)
Hemodialysis	3/19 (16)
Patient past history	
Post-percutaneous coronary intervention (stent)	2/25 (8)
Post-coronary artery bypass graft	1/25 (4)
Culprit lesion distribution	26
LMT bifurcation	5 (19.2)
RCA (proximal/middle)	7 (26.9)/9 (34.6)
LAD (proximal/middle)	1 (3.8)/1 (3.8)
LCX (proximal/middle)	1 (3.8)/2 (7.7)
Culprit lesion morphometric analysis	(25 sections)†
External elastic laminar area, mm^2	19.4 (12.7–23.9)
Internal elastic laminar area, mm^2	17.2 (10–21)
Lumen area, mm^2	3.2 (1.6–5.4)
Plaque area, mm^2	10.9 (7.6–16.2)
Area stenosis, %	74.9 (64.3–87.7)
Necrotic core area, mm^2	0 (0–0)
Necrotic core area, %	0 (0–0)
Calcification area, mm^2	5.0 (2.8–6.7)
Calcification area, %	44.4 (32.9–51.1)
Circumferential calcification,°	92.8 (60.7–175.7)

Values are n, mean ± SD, n (%), median (interquartile range [IQR]) or n/N (%). *Cases that clinical history is unavailable (6 cases) are excluded. †A culprit section at bifurcation (n = 1) is excluded from the morphometric analysis.

LAD = left anterior descending artery; LCX = left circumflex artery; LMT = left main trunk; RCA = right coronary artery.

METHODS

STUDY POPULATION AND GROSS/RADIOGRAPHIC EXAMINATION. From 1994 to 2020, CVPath Institute has received 1,200 cases of sudden coronary death (SCoD) as the first manifestation of coronary heart disease from the Office of the Chief Medical Examiner (OCME) of the State of Maryland. Sudden coronary death was defined as witnessed sudden unexpected death within 6 h of the onset of symptoms from a stable medical condition or death of a person who had been seen in stable condition <24 h antemortem (unwitnessed) (6). Coronary thrombus was observed

FIGURE 1 Consecutive Sections of the Vessels With CN Located in the RCA

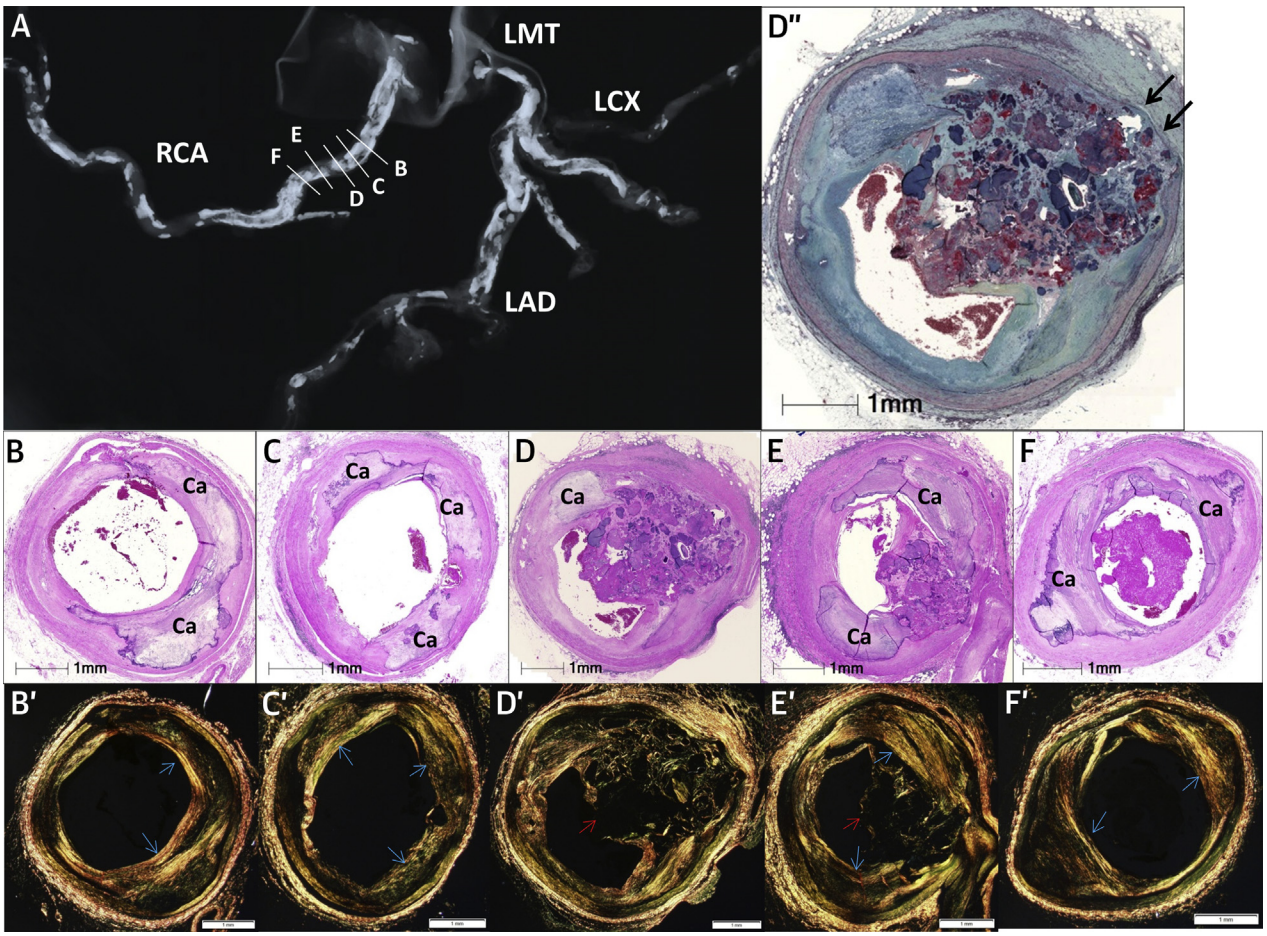

A 79-year-old woman with a past medical history of hypertension, diabetes, coronary artery disease, and congestive heart failure. **(A)** Radiograph demonstrates severe calcification from proximal to mid-portion of the RCA and LAD and left diagonal branches. **Lines B to F** represent the sites of corresponding histological sections. **(B to F)** Low-power images of consecutive severely calcified coronary sections of the RCA stained with hematoxylin and eosin (H&E). **D** (same image as **D"**, stained with Movat Pentachrome) and **E** show the culprit lesion of CN. Medial disruption is seen in **D" (black arrows)**. **B and C** show the proximal, **F** shows the distal, flanking regions adjacent to the culprit lesion **(D, E)**. The flanking sections **(B, C, and F)** show sheet calcification. **B' to F'** are adjacent sections with picrosirius red stain under polarized light. Areas with calcified nodule **(D' and E')** do not demonstrate the presence of collagen (nonpolarized areas, **red arrows**), whereas areas of sheet calcification **(B', C', E', and F')** show collagen (polarized areas, **blue arrows**). CN = calcified node; LAD = left anterior descending; LCX = left circumflex; LMT = Left main trunk; RCA = right coronary artery.

in 524 cases (44%), and, of these, 19 (3.6%) cases had CN (1 patient had 2 CN lesions), resulting in 20 CN lesions from the registry. However, 6 more cases of CN were included in this report, as they were from the same referral (i.e., OCME, Maryland). Clinical records of each case, including available risk factors, were reviewed. Detailed patient information is shown in Supplemental Table 1. The Institutional Review Board at CVPath Institute approved this study. Details of the gross, radiographic, microcomputed tomographic (microCT), and histological evaluation are provided in the Supplemental Materials.

CLASSIFICATION OF LESIONS AND MORPHOLOGIC ANALYSIS. A detailed classification and analysis of lesions are described in the Supplemental Materials. Histological sections from cases with CNs were classified according to our modified American Heart Association classification as previously described (2,22). CN is defined as a lesion with fibrous cap disruption from eruptive calcific nodules associated with an occlusive or nonocclusive platelet/fibrin thrombus (2,11,22-24). Detailed characteristics and morphologic assessments of culprit site and adjacent proximal and distal sections, as well as nonculprit arteries, were

FIGURE 2 Co-Registration Between Radiograph, MicroCT With Histology of CN

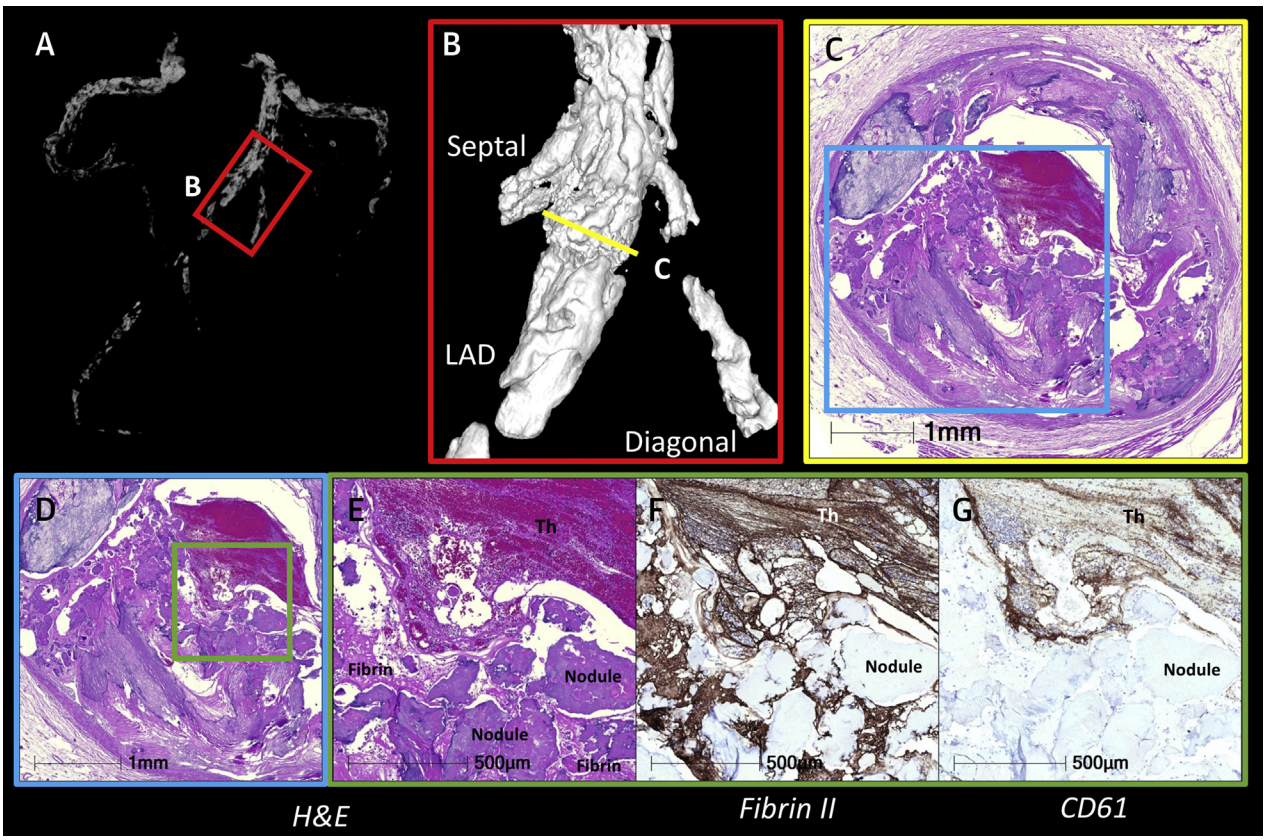

Co-registration between radiograph, microCT with histology for the histologic characterization of CN. **(A)** The radiograph shows diffuse calcification in all 3 coronary arteries. **(B)** MicroCT image of the **red-boxed area** in **(A)** demonstrates severe calcification of LAD, as well as septal and diagonal branches. Low **(C and D [blue boxed area in (C)])** and high **(E [green boxed area in (D)])** power images of a CN stained with H&E showing eruptive CNs with superimposed luminal thrombus (Th). Thrombus stained with antibodies in the **green boxed area** in **(D)** directed against fibrin II **(F)** and CD61 **(G)**. Abbreviations as in Figure 1.

assessed. Morphologic variants of calcification were classified according to size, as previously described (25). In brief, microcalcification was identified by calcium particles ranging from ≥0.5 μm and <15 μm in diameter; punctate calcification >15 μm but <1 mm; and fragment calcification ≥1 mm. More extensive dense sheets of calcification were identified when involving >1 quadrant of the vessel circumference or >3 mm in circumferential dimension. Nodular calcification is the least common form of calcification in the coronary vasculature, but it cannot be distinguished by radiography alone. It is composed of areas of nodular calcification of varying sizes (determined after decalcification), often accompanied by fibrin with a thick, intact fibrous cap. Evidence of fibrous cap disruption is absent in nodular calcification, whereas, in CN, a disruption of the fibrous cap is observed with an absence of endothelium, and there is an overlying platelet/fibrin thrombus. In addition to the classification mentioned previously, we divided sheet calcification into 2 types following the decalcification of arteries: staining by picrosirius red staining and visualization under polarized light. Calcification without evidence of collagen can occur within an area of a NC and is thus called NC calcification, and when calcification involves collagen, it is called collagen (C) calcification. Quantitative morphometry of lesions containing calcified nodules was performed using computerized planimetry (ZEN2, Carl Zeiss, Oberkochen, Germany) as previously described (26).

STATISTICAL ANALYSIS. Results for continuous variables with normal distribution were expressed as mean ± SD. Normality of distribution was tested by the Shapiro-Wilk test. Variables with non-normal distribution were expressed as median (25th to 75th percentiles). Categorical data were analyzed by chi-square test or by Fisher exact tests. Student's *t*-test was used to analyze the significance of differences for

FIGURE 3 **Prevalence of Various Types of Calcification Morphologies in Culprit and Nonculprit Arteries in the LMT, LAD, LCX, and RCA in Subjects With CN**

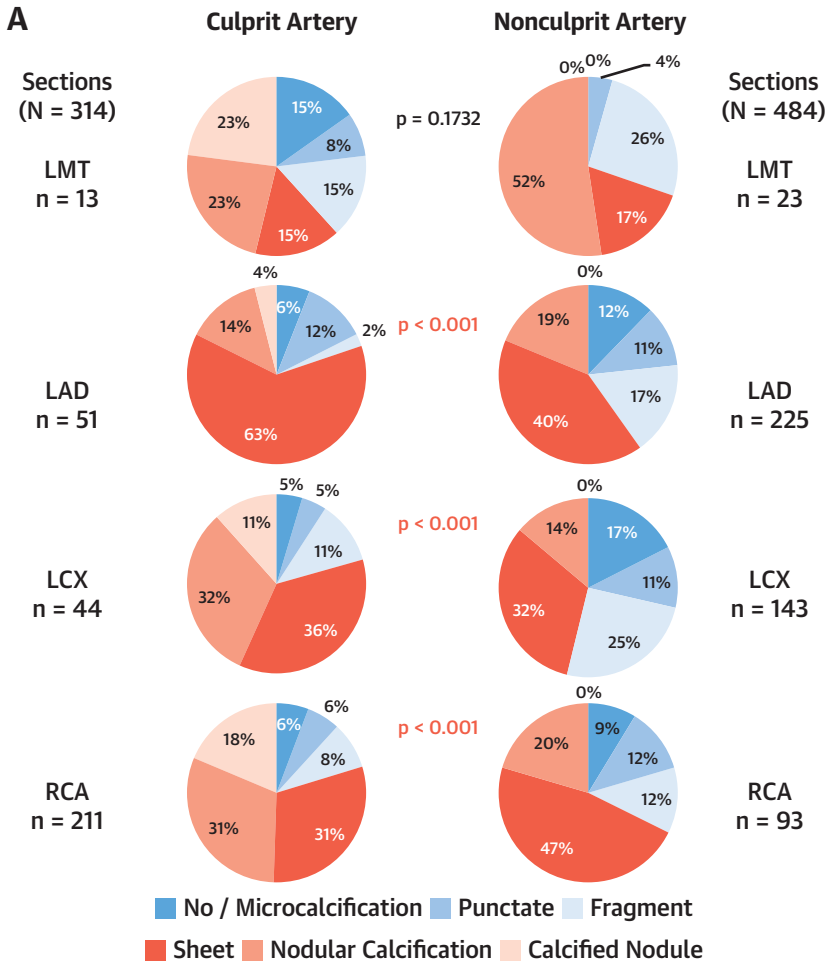

Culprit arteries demonstrate more advanced calcification morphologies such as sheet calcification, nodular calcification, and CN compared with nonculprit arteries. Abbreviations as in Figure 1.

continuous variables with normal distribution. On the other hand, comparisons of variables with nonparametric distribution were performed by the Kruskal-Wallis test, followed by the Steel-Dwass test for multiple comparison for paired observations. A p value of <0.05 was considered statistically significant. JMP software version 13.0 (SAS, Cary, North Carolina) was used for statistical analyses.

RESULTS

DEMOGRAPHICS OF INDIVIDUALS WITH CULPRIT LESION IDENTIFIED AS CN. There was a total of 26 histologic lesions with CN belonging to 25 subjects (Table 1). Of the 25 cases of CN, 20 had sudden death and in 19 it was the first manifestation of heart disease, 1 died of pulmonary embolism and had CN, whereas 2 had histories of percutaneous coronary intervention with stenting, 1 had a history of coronary artery bypass grafting, 1 had cerebral stroke and CN at autopsy, and 1 patient presented with acute myocardial infarction and died 1 day later. Of the 25 cases, 12 were witnessed (7 occurred in the hospital), and the rest (n = 13) were unwitnessed deaths (for details, see Supplemental Table 1). The mean age at the time of death was 70 years, and gender was equally distributed. More than one-half of the subjects with CN had diabetes mellitus (DM) and chronic kidney disease (CKD), with 3 subjects on maintenance hemodialysis. More than 60% of culprit

FIGURE 4 Histologic Appearance of Sheet Calcium in Necrotic Core and Collagen Calcification in Various Atherosclerotic Lesions, Including CN

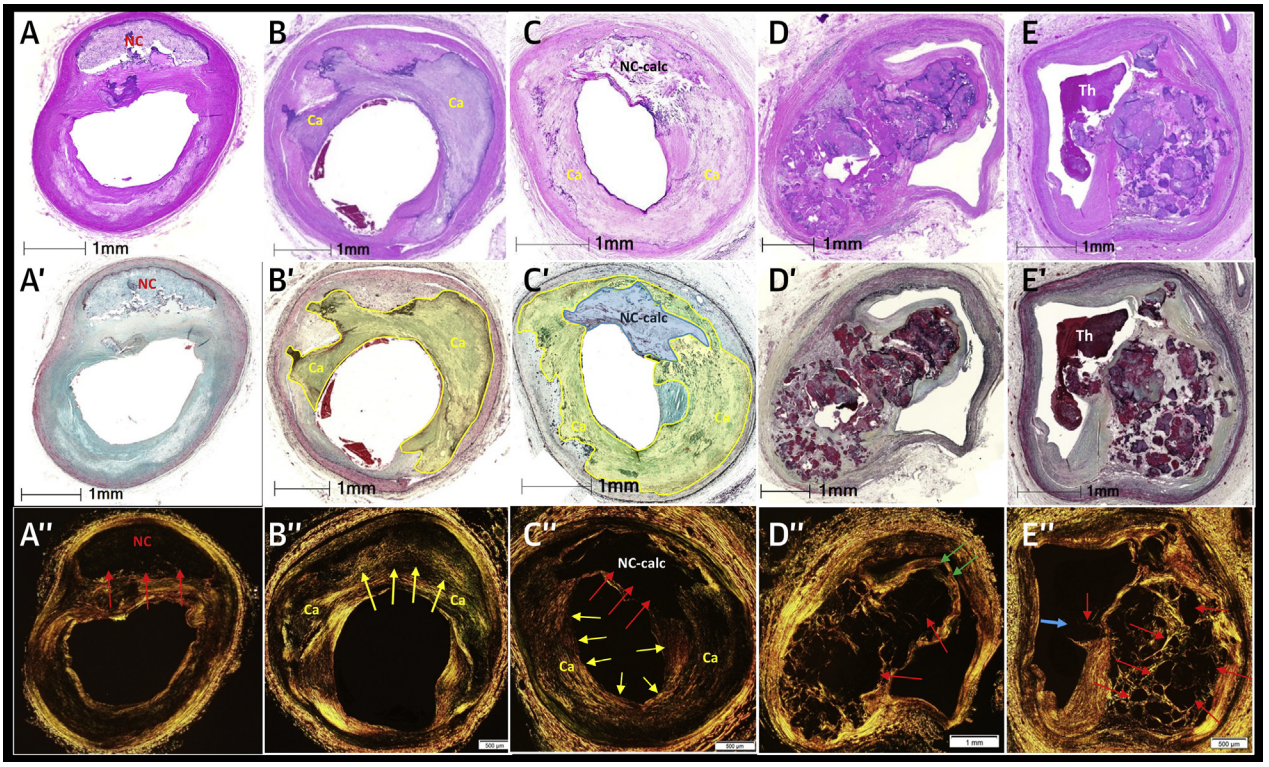

Necrotic core in a fibroatheroma **(A, A')**. The absence of any staining within the necrotic core in picrosirius red stain under polarized light **(red arrows) (A")**. Collagen calcification in a fibrocalcific plaque **(B, B')**, the **purple area (B)** in H&E and the **yellow-green area** in Movat stain **(B')** show sheet calcification. Note that in picrosirius red stain under polarized light, the underlying plaque is composed of collagen **(yellow arrows) (B")**. Necrotic core (NC) calcification **(C, C', C")** is observed and the outer rim of the necrotic core is surrounded by smooth muscle cells and collagen with calcification of both regions. Picrosirius red stain under polarized light shows absence of any staining within the necrotic core region **(red arrows)**, but collagen **(yellow arrows)** is seen in the surrounding calcified area **(C")**. Nodular calcification (healed calcified nodule) **(D, D')**, calcified nodule (CN) **(E, E')**, with corresponding picrosirius red stained sections under polarized light **(D", E")**. Note absence of collagen staining in regions of the nodules **(red arrows)**. Nodular calcification has a healed fibrous cap **(green arrows)**, while CN has a luminal thrombus with an absence of fibrous cap **(blue arrow)**. **Top row** stained with H&E stain, **middle row** stained with Movat stain, and the **third row** stained with picrosirius red under polarized light.

TABLE 2 Comparison of Morphometric Analysis Between Culprit Versus Nonculprit Arteries in Cases With CN

	Culprit Artery	Nonculprit Artery	p Value
Number of vessels evaluated*	26	66	
Number of sections evaluated	313	477	
EEL, mm^2	14.8 (10.9-20.3)	11.4 (8.1-16.3)	<0.0001
IEL, mm^2	12.7 (9.1-17.8)	9.8 (6.9-14.3)	<0.0001
Lumen area, mm^2	4.5 (2.9-7.1)	3.8 (2.2-5.9)	<0.0001
Plaque area, mm^2	7.6 (5.4-10.9)	5.6 (3.7-8.2)	<0.0001
Area stenosis, %	61.1 (49.1-72.5)	57.6 (43.5-71.5)	0.0206
Necrotic core size, mm^2	0 (0-0)	0 (0-0)	0.5592
Necrotic core area, %	0 (0-0)	0 (0-0)	0.5213
Calcification area, mm^2	2.5 (1.1-4.7)	1.4 (0.3-3.3)	<0.0001
Calcification area, %	35.7 (17.7-52.9)	24.5 (6.1-49.3)	0.0001

Values are median (interquartile range) or n. *Sections at bifurcation (n = 6 in culprit vessel and n = 7 in nonculprit vessel) were excluded from the morphometric analysis.

CN = calcified nodule; EEL = external elastic lamina; IEL = internal elastic lamina.

lesions of CN were located in the right coronary artery (RCA) (n = 16), with 9 of those located in the middle and the others located in the proximal region of the artery. Five of 26 culprit lesions were located in the bifurcation of the left main trunk (LMT) (Table 1). Healed myocardial infarction was observed in 19 cases and acute in 4 cases. In 21 cases, the myocardial infarction territory corresponded with the culprit artery with CN (for details, see Supplemental Table 1).

RADIOGRAPHIC AND HISTOPATHOLOGIC CHARACTERISTICS OF CN. Radiographic images of the heart demonstrated severe (>20%) calcification of the coronary arteries in all cases (Supplemental Table 2). Histologically, all CNs demonstrated a luminal fibrin/platelet thrombus, consisting of multiple nodular fragments of calcification penetrating

FIGURE 5 Prevalence of NC Calcification and C Calcification of Sections From Culprit (With Calcified Nodule) and Nonculprit (Proximal and Distal) Arteries Without CN

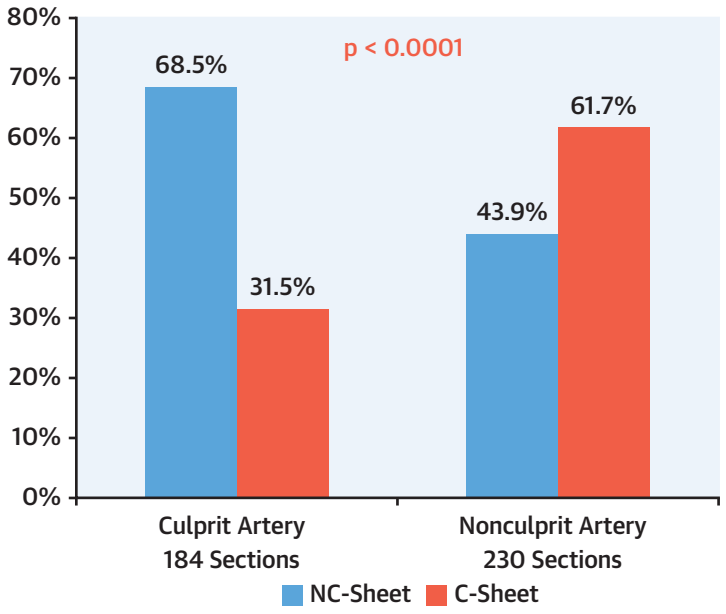

Note that necrotic core (NC) calcification is more prominent in culprit artery sections compared with nonculprit artery sections. Sections that contain sheet calcification were analyzed. C calcification = collagen calcification.

the overlying fibrous cap and protruding into the luminal space, with evidence of endothelial cell loss. The underlying plaques of the eruptive CNs were mainly eccentric, with predominantly nonocclusive thrombi (Supplemental Table 2). The fragmented nodules also often disrupted the underlying medial wall (64%) (**Figure 1**). The median percentage of intimal area occupied by calcification was 44.4% (IQR: 32.9% to 51.2%). NCs were rarely observed (**Table 1**). Immunohistochemical staining demonstrated prominent fibrin surrounding eruptive CNs, with fewer platelet aggregations interspersed (**Figure 2**).

TYPES OF CALCIFICATION AND MORPHOMETRIC ANALYSIS IN CULPRIT AND NONCULPRIT VESSELS. There was a total of 26 arteries that demonstrated a presence of CN, and these are called culprit arteries; all other arteries (n = 66) are nonculprit arteries. From a total of 92 vessels, 803 sections (319 culprit and 484 nonculprit) were examined from 26 lesions with CN. More advanced types of calcification were frequently seen in the culprit vessels with a significantly greater percentage of CN, nodular calcification, and sheet calcium compared with nonculprit vessels (**Figure 3**).

Culprit artery sections demonstrated positive remodeling (internal elastic lamina area of culprit versus nonculprit, median [interquartile range (IQR)], 12.7 mm^2 [9.1 to 17.8 mm^2] vs. 9.8 mm^2 [6.9 to 14.3 mm^2], $p < 0.0001$) with larger plaque area (7.6 mm^2 [5.4 to 10.9 mm^2] vs. 5.6 mm^2 [3.7 to 8.2 mm^2] respectively, $p < 0.0001$) (**Table 2**). The percentage of intimal area occupied by calcification was significantly higher in culprit than in nonculprit artery sections (median [IQR], 35.7% [17.7% to 52.9%] vs. 24.5% [6.1% to 49.3%], respectively, $p = 0.0001$) (**Table 2**).

Picrosirius red staining, followed by examination under polarized light, showed collagen matrix in C-calcification, whereas there was an absence of collagen matrix in NC calcification (**Figure 4**). The prevalence of NC calcification was significantly greater ($p < 0.0001$) in culprit than in nonculprit artery sections (**Figure 5**), suggesting that CNs are likely formed from a breakdown of calcified NCs and not from a breakdown of collagen-rich calcification.

DIFFERENCE BETWEEN CULPRIT SITE HISTOLOGICAL SECTIONS AND ADJACENT PROXIMAL AND DISTAL SECTIONS IN ARTERIES WITH CN. Morphologic features of culprit sections and adjacent proximal and distal

TABLE 3 Comparison of Morphometric Analysis Between Culprit Versus Adjacent Proximal/Distal Sections in Cases With CN

	Proximal	Culprit	Distal	p Value
Number of sections evaluated	21	21	21	
EEL, mm^2	17.4 (11.9–22.3)	19.4 (12.7–23.1)	16.7 (13.4–20.3)	0.8693
IEL, mm^2	14.6 (10.7–19.8)	17.2 (10.0–20.1)	15.3 (11.0–18.1)	0.8417
Lumen area, mm^2	4.3 (2.8–7.4)	3.2 (1.6–5.4)	5.0 (2.9–6.3)	0.1692
Plaque area, mm^2	7.7 (5.7–13.4)	10.9 (7.6–16.2)	9.6 (6.1–12.7)	0.231
Area stenosis, %	69 (53.0–76.1)	77 (64.8–87.7)	64.7 (49.5–76.6)	0.0703
Total calcification area, mm^2	2.4 (1.5–7.2)	4.9 (2.8–6.6)	3.6 (2.0–5.4)	0.1573
Total calcification area, %	29.6 (15.9–56.2)	44.4 (32.2–51.2)	28.0 (18.9–53.0)	0.2328
NC calcification area, mm^2	1.0 (0.4–1.5)	3.7 (2.1–5.2)	1.0 (0.2–2.9)	0.0003
Percent NC calcification area, %	8.6 (4.2–16.7)	28.0 (21.5–38.3)	9.0 (2.1–21.5)	<0.0001
C calcification area, mm^2	1.6 (1.1–3.1)	0.8 (0.6–2.0)	1.6 (0.9–3.0)	0.0613
Percent C calcification area, %	15.1 (7.1–35.1)	10.1 (6.1–15.6)	15.6 (7.9–28.2)	0.0937
Circumferential calcification, °	205.8 (156.7–268.9)	88.9 (54.0–177.2)	239.6 (178.0–332.5)	0.0005

Values are n or median (interquartile range). Heart without consecutive vessel section (n = 4), or post-stent implantation (n = 1) were excluded.
C calcification = collagen calcification; CN = calcified nodule; EEL = external elastic lamina; IEL = internal elastic lamina; NC = necrotic core.

sections, which were within 10 mm from the culprit site, were compared. Hearts without consecutive vessel sections (N = 4) or post-stent implantation (N = 1) were excluded from this analysis. A total of 21 sections were evaluated. The external elastic lamina, internal elastic lamina, and plaque area in culprit site sections were not significantly different than in adjacent proximal and distal sections (Table 3). On the other hand, the degree of circumferential calcification was significantly less in the culprit sections (median [IQR], 89° [54° to 177°]) compared with the adjacent proximal (206° [157° to 269°], p = 0.0034) and distal (240° [178° to 333°], p = 0.0004) nonculprit sections (Table 3, Figure 6). However, the total percentage of calcification, although greater, was not significantly different between culprit sections (median [IQR], 44.4% [32.2% to 51.2%]) and the adjacent proximal and distal sections (29.6% [15.9% to 56.2%], 28.0% [18.9% to 53.0%], respectively, p = 0.23) (Table 3). However, the area of NC calcification was significantly greater in culprit sections (median: 28.0% [IQR: 21.5% to 38.3%]) than in the adjacent proximal (median: 8.6% [IQR: 4.2% to 16.7%], p = 0.009) and distal nonculprit sections (median: 9.0% [IQR: 2.1% to 21.5%], p = 0.008) (Figure 7).

MicroCT ANALYSIS OF ADDITIONAL CASES OF CN. In 3 cases, radiographs, microCT images, and corresponding histological sections were assessed to demonstrate the longitudinal appearance of the culprit lesion and proximal and distal flanking regions. These cases were from subjects 62, 67, and 80 years old (2 men, 1 woman). Two subjects had type 2 DM, 1 had renal failure and was receiving hemodialysis, and all were hypertensive. Postmortem coronary angiography had been performed in 2 cases, and all had radiographic evidence of >20% coronary calcification. The culprit artery was the RCA in 2 and the left anterior descending in 1. MicroCT showed CNs at culprit sites, with the proximal and distal sites

FIGURE 6 Box-and-Whisker Plots Showing Degree of Circumferential Sheet Calcification in the Proximal, Culprit, and Distal Sections of CN

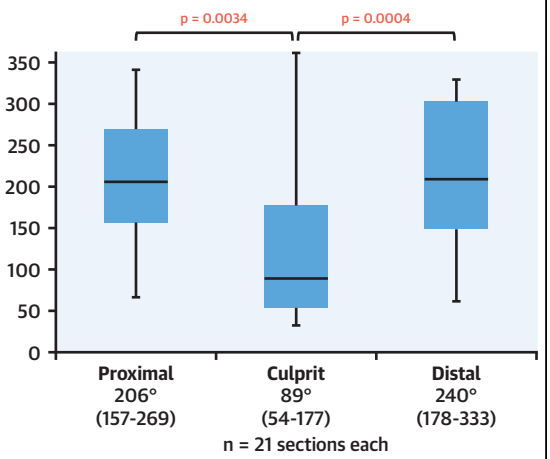

Lines within boxes represent median values. The **upper and lower lines of the boxes** represent the 75th and 25th percentiles, respectively; the upper and **lower bars outside the boxes** represent the maximum and minimum values, respectively. Hearts without consecutive vessel sections (n = 4) or post-stent implantation (n = 1) were excluded. Proximal and distal sheet calcium degree measurements are taken from the area showing the highest degree of calcification within 1 cm (1 to 3 sections) from the culprit site.

showing circumferential or nearly circumferential C calcification (Figure 8). The longitudinal views of microCT clearly showed that the flanking proximal and distal regions contained calcified sheets, with the middle culprit site showing the presence of CN. The flanking regions in 2 cases showed 360° circumferential C calcification, and the third case had C calcification less than three-quarters in circumference.

DISCUSSION

To the best of our knowledge, this study for the first time details the morphology (light microscopy and microCT) and potential sequence of lesion progression that results in calcified nodules, the plaque morphology least frequently associated with coronary thrombosis. Although this type of lesion was first reported by us in 2000 (2), no detailed analysis of the culprit site or the proximal and distal segments has been reported nor was it possible to assess risk factors, as the number of cases was too few. CNs occur in older persons (>60 years) with a similar prevalence in women and men and are associated with comorbidities such as DM and CKD. These findings are consistent with the previous study (18). CNs are predominantly found in the proximal to mid-portions of highly calcified tortuous right coronaries and in bifurcating regions of the left main coronary arteries. The examinations of serial sections from regions proximal and distal to the culprit site show a greater area and arc of C calcification compared with culprit sites of CNs; the area of NC calcification is greater in the culprit sites of CNs. We hypothesize that CNs represent previous sites of eccentric plaque, with NCs that calcify and lack tensile strength owing to an absence of underlying collagen, whereas the flanking regions of sheet calcium are composed of collagen matrix, lending greater strength (21,27).

Most of the CNs were seen in the proximal to middle RCA and in LMT bifurcation. Proximal to middle regions of RCA show a hinge motion or excessive torsion during the cardiac cycle (21,28,29). LMT bifurcation segments tend to show larger NC volumes (30). In these locations, there was eccentric calcification sandwiched between flanking proximal and distal plaques with heavy or concentric calcification. The hypothesis that an absence of underlying structural components (i.e., collagen) contributing to the formation of CNs is reminiscent of strut fractures observed in coronary drug-eluting stents. The fractures occur more frequently in segments adjacent to "overlapping" regions in which the stiffest regions are the overlapping stents lying adjacent to the more pliable, nonoverlapped stented segments, which are often the site of stent fracture (31,32). These results indicate that heavily calcified coronary segments lie directly adjacent to more flexible regions and that these less calcified segments are more susceptible to external mechanical forces because of greater movement of the coronary artery during the cardiac cycle, thus leading to CN (Central Illustration). We assume similar mechanisms likely occur for both CN and nodular calcification areas. More recently, Lee et al. demonstrated that lesions with nodular calcification show a greater change in the angiographic angle between systole and diastole (21), which is consistent with our interpretation.

Although the etiology of plaque calcification continues to be debated, most agree that the progression of calcification in advanced atheromatous plaques begins as an extension from the outer rim of the NC with extension that involves surrounding smooth muscle cells and collagen-rich matrix (23,24,33). Further, lesion progression occurs when the central NC becomes confluent with sheets of calcification extending in the longitudinal direction, recognized as

FIGURE 7 Percent Area of C Calcification and NC Calcification of Culprit Section and Adjacent Proximal and Distal Section in Patients With CN

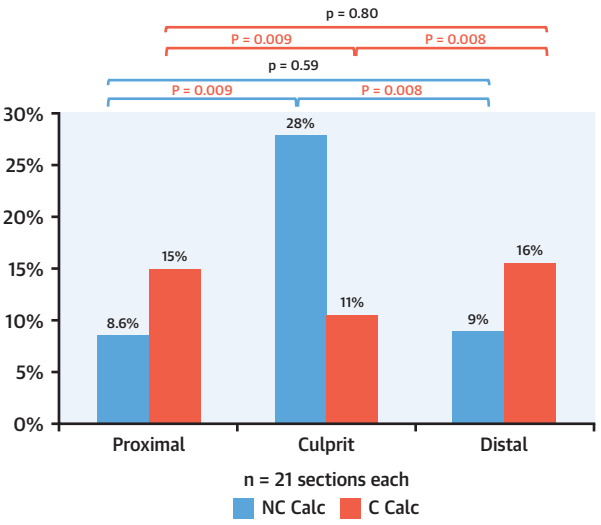

Note that the area of NC calcification is greater in the culprit section compared with adjacent proximal and distal sections; in contrast, the C calcification is greater in proximal and distal nonculprit sections compared with culprit site sections. Hearts without consecutive vessel section (n = 4) or post-stent implantation (n = 1) were excluded. Proximal and distal sections are taken from the maximum value within 1 cm (1 to 3 sections) from the culprit site. Abbreviations as in Figures 3 and 5.

FIGURE 8 Angiogram, Fluoroscopy, Radiograph, MicroCT Images of CN With Adjacent Flanking Sections and Corresponding Histological Sections

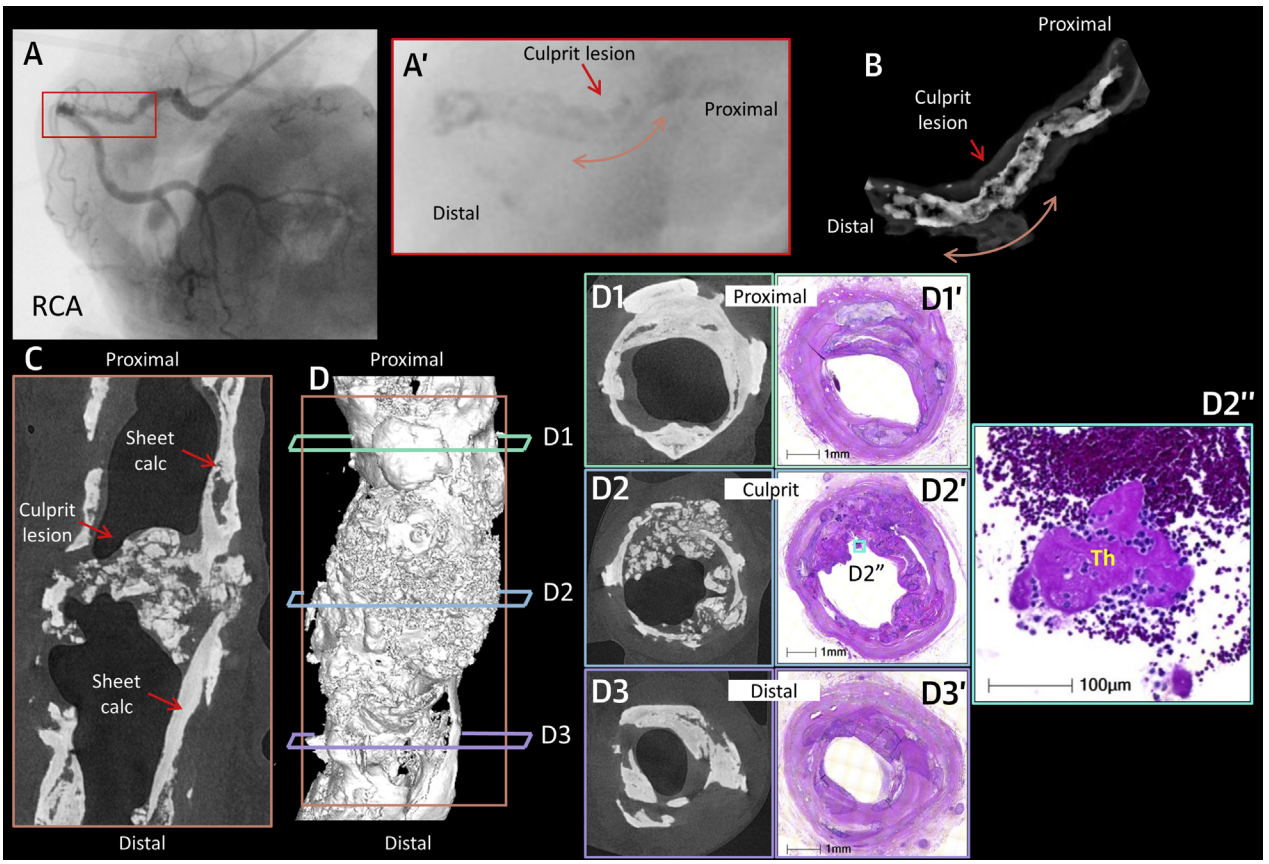

A 62-year-old woman with a past medical history of hypertension, dialysis-dependent renal failure, and a history of smoking. Postmortem angiogram **(A)** and fluoroscopy **(A', red-boxed area in A)** demonstrated tortuous proximal RCA with severe stenosis and calcification. Radiograph from the region of the culprit site following removal from the heart shows severe calcification of the RCA **(B)**. MicroCT of the longitudinally bisected half of the right coronary artery **(C)**, and corresponding 3-dimensional whole artery microCT showing only calcification **(D)**. **Lines D1 to D3 in D** represent the sites of corresponding histological sections. **D1 to D3** are microCT and the corresponding histological cross-sections (**D1' to D3'** H&E stain) from culprit sites **(D2, D2')** and proximal **(D1, D1')** and distal **(D3, D3')** flanking sections. **D2"** is a high-power image of the **blue boxed area** in **D2'**, showing fibrin-platelet thrombus attachment at the culprit lesion of CN. Abbreviations as in Figure 1.

the fibrocalcific plaque. In our study, there was an absence of collagen fibers within areas of nodular calcification, as recognized by picrosirius red staining, which appears similar to late NC. Therefore, we hypothesize that CN is an extension of fragmented NC calcification rather than the hard, sheet calcification more commonly associated with areas composed of collagen-rich fibrous tissue.

Calcium fragmentation resulting in nodule formation likely elicits intraplaque hemorrhage caused by damage of the surrounding capillaries and arterioles, as well as the formation of clots involving accumulated fibrin and red blood cells. Hemosiderin deposition with macrophage infiltration may also be observed, depending on the duration of the CN. Intraplaque hemorrhage is observed in 40% of culprit CN lesions, highly suggestive of capillary breaks occurring during calcium fragmentation. Although the current study cannot confirm a predisposition toward disruption of a thin fibrous cap, mechanical force exerted by the calcified fragments is likely the underlying mechanism causing the discontinuity of the overlying cap, along with the loss of surface endothelium and overlying platelet/fibrin thrombus.

Recent imaging studies involving IVUS or OCT have shed more light on CN plaque morphology (15-21). These studies demonstrated that the incidence of CN is 2.5% to 8.0%. However, a detailed

CENTRAL ILLUSTRATION **Proposed Mechanism of the Occurrence of Calcified Nodule**

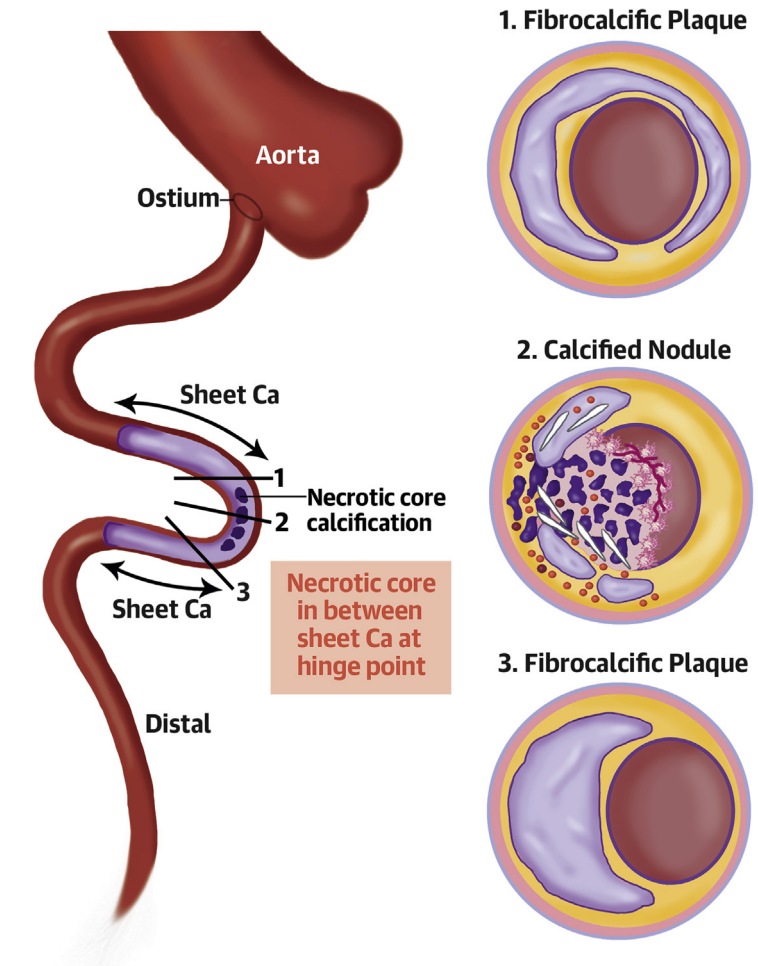

Torii, S. et al. J Am Coll Cardiol. 2021;77(13):1599-611.

Middle segment of right coronary artery is more susceptible to external mechanical forces caused by greater movement of the coronary artery during the cardiac cycle. Heavily calcified coronary segments—fibrocalcific plaque, the arc of calcification is large—**(1, 3)** which contain large amounts of rigid collagen calcification, lie directly adjacent to more flexible (less tensile strength; the arc of calcification is small) lesion containing necrotic core calcifications. The necrotic core calcium fragments into multiple pieces, causing capillary breaks and intraplaque hemorrhage, increasing plaque volume that eventually protrudes into the lumen, disrupting the fibrous cap and overlying endothelium, forming calcified nodules or nodular calcification areas.

assessment of the CN by histology was lacking until the current study. Three of our subjects underwent microCT, and the longitudinal images are suggestive of the mechanism by which CNs form. Although thrombus is a key discriminator for the detection of CN in OCT and IVUS, the clinical definition of CN recognized by imaging devices has been inconsistent in terms of whether or not thrombus

attachment is essential. In light of this, most studies are reporting on nodular calcification with an intact fibrous cap, which is commonly observed in heavily diseased coronary, peripheral, and carotid arteries. From our SCoD cases, the attachment of a surface thrombus is a prerequisite for the identification of the CN, which is recognized as a rare cause of acute coronary thrombus (2).

STUDY LIMITATIONS. The current study is limited to autopsy cases of SCoD; therefore, our findings may not apply to surviving patients with ACS. Moreover, although we have evaluated all cases of CN from our registry of >1,000 SCoDs from the Maryland OCME, spanning over 20 years, there could be a selection/referral bias. In addition, detailed patient information—including past medical history, medications, laboratory tests, and degree of calcification of the other arteries— was not available in most of the cases. Nonetheless, our study details—for the first time—a relatively large series of histologically documented cases of CN from an established autopsy registry of SCoD, along with potential mechanistic insight into its occurrence. Finally, microCT was available in limited cases (3 of the 25 cases). MicroCT is preformed before decalcification and therefore better defines the exact location and the type of calcium in 3-dimensional views—that is, longitudinal and cross-sectional—therefore allowing us to allude the mechanism of calcified nodule with histologic support of our hypothesis.

CONCLUSIONS

The CN, the rarest form of coronary thrombosis, mainly occurs in older persons, with a median age of 70 years and equal gender distribution, and there is a high prevalence of DM and CKD in these subjects. These lesions mainly develop in the proximal to mid-portions of highly tortuous right coronary arteries, where the range of hinge motion of the coronary artery is maximal. The mechanism of fibrous cap disruption and thrombosis is hypothesized to be initiated through the fragmentation of calcified NCs, and the culprit plaque develops between flanking areas of stable fibrocalcific plaques (collagen calcification) in coronary arteries in which hinge motion or excessive torsion is seen. Our detailed histological characterization of CNs at autopsy provides an important understanding of a uniquely uncommon cause for acute coronary thrombosis. As the population ages, and considering the rise in DM caused by obesity, the incidence of CN is likely to rise as well, and we will need greater awareness of its occurrence and pathophysiology to prevent its fatal thrombotic complications.

FUNDING SUPPORT AND AUTHOR DISCLOSURES

Dr.Torii has received research grants from Sunrise Laboratories. CVPath Institute has received institutional research support from NIH-HL141425, Leducq Foundation Grant, 480 Biomedical, 4C Medical, 4Tech,Abbott, Accumedical, Amgen, Biosensors, Boston Scientific, Canon USA, Cardiac Implants, Celonova, Claret Medical, Concept Medical, Cook, CSI, DuNing, Inc, Edwards LifeSciences, Emboline, Endotronix, Envision Scientific, Lutonix/Bard, Gateway, Lifetech, Limflo, MedAlliance, Medtronic, Mercator, Merill, Microport Medical, Microvention, Mitraalign, Mitra Assist, NAMSA, Nanova, Neovasc, NIPRO, Novogate, Occulotech, OrbusNeich Medical, Phenox, Profusa, Protembis, Qool, ReCor Medical, Senseonics, Shockwave, Sinomed, Spectranetics, Surmodics, Symic, Vesper, W.L. Gore, and Xeltis. Dr. Finn has received honoraria from Abbott Vascular, Biosensors Boston Scientific, Celonova, Cook Medical, CSI, Lutonix Bard, Sinomed, and Terumo Corporation; and is a consultant to Amgen, Abbott Vascular, Boston Scientific, Celonova, Cook Medical, Lutonix Bard, and Sinomed. Dr. Cornelissen has received research grants from University Hospital RWTH Aachen. Dr. Virmani has received honoraria from Abbott Vascular, Biosensors, Boston Scientific, Celonova, Cook Medical, Cordis, CSI, Lutonix Bard, Medtronic, OrbusNeich Medical, CeloNova, SINO Medical Technology, ReCor, Terumo Corporation, W. L. Gore, and Spectranetics; and has served as a consultant to Abbott Vascular, Boston Scientific, Celonova, Cook Medical, Cordis, CSI, Edwards Lifesciences, Lutonix Bard, Medtronic, OrbusNeich Medical, ReCor Medical, Sinomededical Technology, Spectranetics, Surmodics, Terumo Corporation, W. L. Gore, and Xeltis. All other authors have reported that they have no relationships relevant to the contents of this paper to disclose.

ADDRESS FOR CORRESPONDENCE: Dr. Renu Virmani, CVPath Institute, Inc., 19 Firstfield Road, Gaithersburg, Maryland 20878, USA. E-mail: rvirmani@cvpath.org.

PERSPECTIVES

COMPETENCY IN MEDICAL KNOWLEDGE: Fragmentation of the necrotic core of calcified coronary atherosclerotic plaque nodules (CN) promotes fibrous cap disruption and luminal thrombosis, which could lead to acute ischemic syndromes and some cases of sudden death.

TRANSLATIONAL OUTLOOK: Understanding the pathophysiological role of CN in coronary plaque disruption is needed to develop clinical management strategies that prevent thrombotic complications.

REFERENCES

1. Benjamin EJ, Virani SS, Callaway CW, et al. Heart disease and stroke statistics-2018 update: a report from the American Heart Association. Circulation 2018;137:e67–492.

2. Virmani R, Kolodgie FD, Burke AP, Farb A, Schwartz SM. Lessons from sudden coronary death: a comprehensive morphological classification scheme for atherosclerotic lesions. Arterioscler Thromb Vasc Biol 2000;20:1262–75.

3. Yahagi K, Davis HR, Arbustini E, Virmani R. Sex differences in coronary artery disease: pathological observations. Atherosclerosis 2015;239:260–7.

4. Narula J, Nakano M, Virmani R, et al. Histopathologic characteristics of atherosclerotic coronary disease and implications of the findings for the invasive and noninvasive detection of vulnerable plaques. J Am Coll Cardiol 2013;61:1041–51.

5. Schaar JA, Muller JE, Falk E, et al. Terminology for high-risk and vulnerable coronary artery plaques. Report of a meeting on the vulnerable plaque, June 17 and 18, 2003, Santorini, Greece. Eur Heart J 2004;25:1077–82.

6. Farb A, Tang AL, Burke AP, Sessums L, Liang Y, Virmani R. Sudden coronary death: frequency of active coronary lesions, inactive coronary lesions, and myocardial infarction. Circulation 1995;92:1701–9.

7. Burke AP, Farb A, Malcom GT, Liang YH, Smialek J, Virmani R. Coronary risk factors and plaque morphology in men with coronary disease who died suddenly. N Engl J Med 1997;336:1276–82.

8. van der Wal AC, Becker AE, van der Loos CM, Das PK. Site of intimal rupture or erosion of thrombosed coronary atherosclerotic plaques is characterized by an inflammatory process irrespective of the dominant plaque morphology. Circulation 1994;89:36–44.

9. Farb A, Burke AP, Tang AL, et al. Coronary plaque erosion without rupture into a lipid core: a frequent cause of coronary thrombosis in sudden coronary death. Circulation 1996;93:1354–63.

10. Virmani R, Burke AP, Farb A. Plaque rupture and plaque erosion. Thromb Haemost 1999;82:1–3.

11. Virmani R, Burke AP, Farb A, Kolodgie FD. Pathology of the vulnerable plaque. J Am Coll Cardiol 2006;47:C13–8.

12. Schwartz RS, Burke A, Farb A, et al. Microemboli and microvascular obstruction in acute coronary thrombosis and sudden coronary death: relation to epicardial plaque histopathology. J Am Coll Cardiol 2009;54:2167–73.

13. Kramer MC, Rittersma SZ, de Winter RJ, et al. Relationship of thrombus healing to underlying plaque morphology in sudden coronary death. J Am Coll Cardiol 2010;55:122–32.

14. Kolodgie FD, Burke AP, Farb A, et al. Differential accumulation of proteoglycans and hyaluronan in culprit lesions: insights into plaque erosion. Arterioscler Thromb Vasc Biol 2002;22:1642–8.

15. Lee JB, Mintz GS, Lisauskas JB, et al. Histopathologic validation of the intravascular ultrasound diagnosis of calcified coronary artery nodules. Am J Cardiol 2011;108:1547–51.

16. Xu Y, Mintz GS, Tam A, et al. Prevalence, distribution, predictors, and outcomes of patients with calcified nodules in native coronary arteries: a 3-vessel intravascular ultrasound analysis from Providing Regional Observations to Study Predictors of Events in the Coronary Tree (PROSPECT). Circulation 2012;126:537–45.

17. Higuma T, Soeda T, Abe N, et al. A combined optical coherence tomography and intravascular ultrasound study on plaque rupture, plaque erosion, and calcified nodule in patients with ST-segment elevation myocardial infarction: incidence, morphologic characteristics, and outcomes after percutaneous coronary intervention. J Am Coll Cardiol Intv 2015;8:1166–76.

18. Jia H, Abtahian F, Aguirre AD, et al. In vivo diagnosis of plaque erosion and calcified nodule in patients with acute coronary syndrome by intravascular optical coherence tomography. J Am Coll Cardiol 2013;62:1748–58.

19. Wang L, Parodi G, Maehara A, et al. Variable underlying morphology of culprit plaques associated with ST-elevation myocardial infarction: an optical coherence tomography analysis from the SMART trial. Eur Heart J Cardiovasc Img 2015;16:1381–9.

20. Kajander OA, Pinilla-Echeverri N, Jolly SS, et al. Culprit plaque morphology in STEMI - an optical coherence tomography study: insights from the TOTAL-OCT substudy. EuroInterv 2016;12:716–23.

21. Lee T, Mintz GS, Matsumura M, et al. Prevalence, Predictors, and clinical presentation of a calcified nodule as assessed by optical coherence tomography. J Am Coll Cardiol Img 2017;10:883–91.

22. Yahagi K, Kolodgie FD, Otsuka F, et al. Pathophysiology of native coronary, vein graft, and in-stent atherosclerosis. Nat Rev Cardiol 2016;13:79–98.

23. Mori H, Torii S, Kutyna M, Sakamoto A, Finn AV, Virmani R. Coronary artery calcification and its progression: what does it really mean? J Am Coll Cardiol Img 2018;11:127–42.

24. Otsuka F, Sakakura K, Yahagi K, Joner M, Virmani R. Has our understanding of calcification in human coronary atherosclerosis progressed? Arterioscler Thromb Vasc Biol 2014;34:724–36.

25. Torii S, Mustapha JA, Narula J, et al. Histopathologic characterization of peripheral arteries in subjects with abundant risk factors: correlating imaging with pathology. J Am Coll Cardiol Img 2019;12:1501–13.

26. Torii S, Jinnouchi H, Sakamoto A, et al. Vascular responses to coronary calcification following implantation of newer-generation drug-eluting stents in humans: impact on healing. Eur Heart J 2020;41:786–96.

27. Puentes J, Garreau M, Lebreton H, Roux C. Understanding coronary artery movement: a knowledge-based approach. Artif Intell Med 1998;13:207–37.

28. Nakagawa Y, Hayashi H, Izumi C, et al. Four-dimensional computed tomography-based finite element modeling of the behavior of the right coronary artery. Circ J 2017;81:1059–61.

29. Chinikar M, Sadeghipour P. Coronary stent fracture: a recently appreciated phenomenon with clinical relevance. Curr Cardiol Rev 2014;10:349–54.

30. Nakazawa G, Yazdani SK, Finn AV, Vorpahl M, Kolodgie FD, Virmani R. Pathological findings at bifurcation lesions: the impact of flow distribution on atherosclerosis and arterial healing after stent implantation. J Am Coll Cardiol 2010;55:1679–87.

31. Nakazawa G, Finn AV, Vorpahl M, et al. Incidence and predictors of drug-eluting stent fracture in human coronary artery a pathologic analysis. J Am Coll Cardiol 2009;54:1924–31.

32. Torii S, Jinnouchi H, Sakamoto A, et al. Drug-eluting coronary stents: insights from preclinical and pathology studies. Nat Rev Cardiol 2020;17:37–51.

33. New SE, Goettsch C, Aikawa M, et al. Macrophage-derived matrix vesicles: an alternative novel mechanism for microcalcification in atherosclerotic plaques. Circ Res 2013;113:72–7.

KEY WORDS acute myocardial infarction, calcified nodule, sudden coronary death

APPENDIX For supplemental material and tables, please see the online version of this paper.